

The Hot Gas Environment of the Radio Galaxy 3C 388: Quenching the Accumulation of Cool Gas in a Cluster Core by a Nuclear Outburst

R. P. Kraft

*Harvard/Smithsonian Center for Astrophysics, 60 Garden St., MS-67, Cambridge, MA
02138*

J. Azcona

Observatoire de Paris-Meudon-Nancy, 5 Place Jules Janssen, 92195 Meudon Cedex, France

W. R. Forman

*Harvard/Smithsonian Center for Astrophysics, 60 Garden St., MS-2, Cambridge, MA
02138*

M. J. Hardcastle

*University of Hertfordshire, School of Physics, Astronomy, and Mathematics, Hatfield
AL10 9AB, UK*

C. Jones, S. S. Murray

*Harvard/Smithsonian Center for Astrophysics, 60 Garden St., MS-2, Cambridge, MA
02138*

ABSTRACT

We present results from a 35 ks *Chandra*/ACIS-I observation of the hot ICM around the FR II radio galaxy 3C 388. 3C 388 resides in a cluster environment with an ICM temperature of ~ 3.5 keV. We detect cavities in the ICM coincident with the radio lobes. The enthalpy of these cavities is $\sim 1.2 \times 10^{60}$ ergs. The work done on the gas by the inflation of the lobes is $\sim 3 \times 10^{59}$ ergs, or ~ 0.87 keV per particle out to the radius of the lobes. The radiative timescale for gas at the center of the cluster at the current temperature is a few Gyrs. The gas in the core was probably cooler and denser before the outburst, so the cooling time was considerably shorter. We are therefore likely to be witnessing the quenching of a cluster cooling flow by a radio galaxy outburst. The mechanical power of the lobes is at least 20 times larger than the radiative losses out to the cooling radius.

Outbursts of similar power with a $\sim 5\%$ duty cycle would be more than sufficient to continually reheat the cluster core over the Hubble time and prevent the cooling of any significant amount of gas. The mechanical power of the outburst is also roughly two orders of magnitude larger than either the X-ray luminosity of the active nucleus or the radio luminosity of the lobes. The equipartition pressure of the radio lobes is more than an order of magnitude lower than that of the ambient medium, indicating that the pressure of the lobe is dominated by something other than the relativistic electrons radiating at GHz frequencies.

Subject headings: galaxies: individual (3C 388) - X-rays: galaxies: clusters - galaxies: ISM - hydrodynamics - galaxies: jets

1. Introduction

Our understanding of radio plasma/ISM interactions in radio galaxies has been revolutionized by *Chandra* X-ray Observatory studies of the gaseous atmospheres surrounding these sources. *Chandra* is the first X-ray observatory with spatial resolution sufficient to carry out detailed studies of the shells, bow shocks, bubbles, cavities, cold filaments, and surface brightness discontinuities in the gas that are the consequences of powerful AGN outburst. X-ray studies of the gaseous environments of radio galaxies give us important clues about the dynamics, the energetics, and the temporal evolution of AGN outbursts that cannot be directly obtained from radio observations.

Interest in radio galaxy/ICM interactions has flourished in the *Chandra* era after the realization that the large cluster cooling flows predicted by the earlier generation of X-ray observatories do not exist (Peterson *et al.* 2001; Kaastra *et al.* 2004). Since the radiative cooling time of the gas at the center of many clusters is a few Gyrs or less, the gas must be reheated, either occasionally or continuously, to prevent the formation of large cooling flows. There are several possible sources of energy to reheat the core including cosmic rays (Böhringer & Morfill 1988), thermal conduction from the hot gas halo (Tucker & Rosner 1983; Dolag *et al.* 2004) or supernovae (McNamara *et al.* 2004). The most promising method to reheat cooling cluster cores and balance radiative losses is heating by nuclear outbursts (Tabor & Binney 1993; Churazov *et al.* 2002). In this scenario, there is a cyclical relationship between the cooling gas and the formation of radio galaxies. As the gas cools, it falls in toward the central supermassive black hole, initiating a nuclear outburst. The mechanical energy of the nuclear outflow heats (either via shocks or via conversion of bubble enthalpy to thermal energy of the ambient gas) the ICM (Reynolds, Heinz, & Begelman 2001, 2002). AGN outbursts therefore play a critical role in the evolution of clusters of

galaxies. Occasional outbursts can provide sufficient energy to reheat the radiatively cooling cores of galaxy clusters and prevent large cooling flows from forming.

The radio galaxy 3C 388 is classified as a Fanaroff-Riley type II (FR II) radio galaxy, although its luminosity ($P_{178\text{ MHz}}=5\times 10^{25}\text{ W Hz}^{-1}$ (Fanaroff & Riley 1974)) lies near the FR I/II dividing line. The radio morphology of this source is closer to a ‘fat-double’ (Owen & Laing 1989) than the canonical FR II ‘classical double’ such as Cyg A and 3C 98. Optically, the nucleus of 3C 388 is classified as a low-excitation radio galaxy (Jackson & Rawlings 1997). Multi-frequency VLA observations of 3C 388 show significant structure in spectral index maps which has been interpreted as evidence for multiple nuclear outbursts (Roettiger *et al.* 1994). Previous X-ray observations of this radio galaxy have shown that it is embedded in a cluster environment (Feigelson & Berg 1983; Hardcastle & Worrall 1999; Leahy & Gizani 2001). The local galaxy environment is extremely dense (Prestage & Peacock 1988), and the central elliptical galaxy which hosts 3C 388 is one of the most luminous ($M_B=-24.24$) in the local Universe (Owen & Laing 1989; Martel *et al.* 1999).

In this paper we present results from a 35 ks observation of the hot gas around 3C 388. This paper is organized as follows. Section two contains a summary of the observational details. The results of the data analysis are presented in section 3. We discuss the implications of our results in section 4. Section 5 contains a brief summary and conclusions, as well as possible future observations. We assume WMAP cosmology throughout this paper (Spergel *et al.* 2003). The observed redshift ($z=0.0908$) of the host galaxy of 3C 388 corresponds to a luminosity distance of 410.3 Mpc, and one arcminute is 100.32 kpc. All uncertainties are at 90% confidence unless otherwise stated, and all coordinates are J2000. All elemental abundances in this paper are relative to the Solar value tabulated by Anders & Grevasse (1989). Absorption by gas in our Galaxy ($N_H=6.32\times 10^{20}\text{ cm}^{-2}$) is included in all spectral fits (Dickey & Lockman 1990).

2. Observations

The radio galaxy 3C 388 was observed twice with *Chandra*/ACIS-I in VF mode. The first observation was made on January 9, 2004 (OBSID 4765) for 7.5 ks, and was terminated because of high background. The second observation was made on January 29, 2004 (OBSID 5295) for 32.5 ks. In this paper we present data only from the second observation. The complications of combining the data sets (different instrument roll angles and higher background in the first observation) more than offset the advantage of the additional $\sim 25\%$ observing time. We made light curves for each CCD in the 5.0 to 10.0 keV band to search for background flares and removed intervals where the background rate was more than 3σ

above the mean, leaving 30717.5 s of good data. VF filtering was applied to the data to reduce the background. Bad pixels, hot columns, and columns along node boundaries also were removed, and standard ASCA grade filtering (0,2,3,4,6) was applied to the events file. Diffuse emission from the ICM fills the *Chandra* FOV in this observation, so it was not, in general, possible to use a local background measured in the same observation. Background for both imaging and spectral analysis was estimated using the high latitude deep sky observations provided by the CXC. An image of the ACIS-I FOV smoothed by a Gaussian (6'' r.m.s.) in the 0.5-2.0 keV band is shown in Figure 1.

We use archival VLA observations of 3C 388 at two frequencies, 8.4 GHz and 1.4 GHz, to make X-ray/radio comparisons. Radio spectral index maps of Roettiger *et al.* (1994) show two spatially separated regions in each lobe. Near the radio peaks of each lobe, the spectral indices of the radio flux density ($S_\nu \propto \nu^{-\alpha}$) are between 0.6-0.8. The radio spectral index of the more distant regions is considerably steeper (~ 1.5), with a sharp discontinuity defining these distinct regions. Roettiger *et al.* (1994) argued that the radio lobe is thought to be inflating into the relic lobe of a previous outburst.

3. Analysis

An adaptively smoothed, exposure corrected, background subtracted *Chandra*/ACIS-I image of 3C 388 in the 0.5-2.0 keV band is shown in Figure 2. All point sources with four or more counts, other than the active nucleus of 3C 388, have been removed and replaced by the mean background from an adjacent annulus. Diffuse emission from the cluster gas fills the ACIS-I FOV. Contours from the 1.4 GHz radio map of 3C 388 are overlaid. The radio source is small (1'/100 kpc across) and lies at the center of the cluster. A secondary peak of X-ray emission lies $\sim 4.8'$ (482 kpc) east of the cluster center, and is perhaps associated with a merging subcluster. The X-ray isophotes within $\sim 1'$ of the nucleus are elliptical ($e \sim 0.3$). The major axis of the elliptical isophotes is aligned along the axis of the radio jet, suggesting that the NE/SW extension may be related to the nuclear outburst. On larger scales, however, the isophotes are approximately circular (ignoring the peak to the East). It is likely that the observed ellipticity of the X-ray isophotes is the result of the inflation of the radio lobe as observed in simulations (Basson & Alexander 2003). For simplicity we assume spherical symmetry in our analysis below.

3.1. Radio Lobe/ICM Interaction

Figure 3 contains an adaptively smoothed, background subtracted, exposure corrected *Chandra*/ACIS-I image of the central $1.5' \times 1.1'$ region with 8.4 GHz radio contours overlaid. The X-shaped X-ray morphology, typical of radio plasma/ICM interactions (e.g. M84 (Finoguenov & Jones 2001) and NGC 4636 (Jones *et al.* 2002)), is clearly visible in Figure 3. There are decrements in the X-ray surface brightness coincident with the radio lobes. To enhance the visibility of these decrements, we have subtracted the azimuthally averaged surface brightness profile from Figure 3. The residual image is shown in Figure 4. The inflation of the radio lobes has evacuated cavities in the gas and created the deficits in the X-ray surface brightness.

To constrain the dynamics of the interaction of the radio lobes with the ICM, we fit the X-ray spectra in three groups of regions in the vicinity of the lobes. Two of the groups are shown in Figure 5. The regions outlined in red (combined for spectral analysis) represent the gas in the central region of the cluster, and the two regions in white are coincident with the X-ray cavities created by the inflation of the lobe. A third region (not shown on Figure 5) is an elliptical annulus with inner and outer major axes of $25''$ and $50''$, respectively, with the major axis aligned along the jet. The spectra were fit using a single temperature APEC model and Galactic absorption. The best fit temperatures and elemental abundances for each region are summarized in Table 1 (uncertainties are at 90% confidence). There is no statistically significant evidence for any temperature structure in the regions chosen, although the uncertainties are large enough that the presence of a weak shock cannot be excluded. The absence of gas hotter than the ambient ICM demonstrates that the lobes are not expanding with large Mach number. In addition, there is no evidence for cool rims similar to those seen around cavities in other clusters (e.g. Hydra A (McNamara *et al.* 2000)) that are thought to have been dredged up from the center of the cluster.

3.2. Large Scale X-ray Emission

The azimuthally averaged radial surface brightness profile of the X-ray emission from the gas is shown in Figure 7. The best-fit isothermal β -model profile has been overlaid. We find $\beta=0.444 \pm 0.003$ and a core radius $r_0=8.30'' \pm 0.01''$ from fitting the surface brightness profile between $5''$ and $200''$ from the nucleus, roughly consistent with values previously reported by Leahy & Gizani (2001). There is an excess of emission in the central $5''$ over the best-fit β -model. This is due to a combination of cooling gas in the galaxy core and a contribution from the central AGN (see below).

We fit the temperature in six annuli centered on 3C 388 using an APEC model with Galactic absorption ($N_H=6.32\times 10^{20}$ cm $^{-2}$), excluding the subcluster to the East. The temperature and elemental abundance were free parameters in these fits. Plots of the temperature and elemental abundance as a function of radius from the center of the cluster are shown in Figure 6. The temperature of the gas within $\sim 30''$ of the nucleus (i.e. within the boundary of the radio lobes) is ~ 3 keV. The gas temperature rises slightly beyond the radio lobes to 3.7 ± 0.4 keV, with a weak decline ($T(R) \propto R^{-0.2\pm 0.05}$ at 90% confidence) as a function of projected distance, R , from the nucleus. The X-ray luminosity of the gas within a projected radius of 401.3 kpc (30% of the virial radius (Evrard, Metzler, & Navarro 1996)) is 9.0×10^{43} ergs s $^{-1}$ in the 0.1-10.0 keV band (unabsorbed) assuming the gas is isothermal (3.4 keV - the best-fit emission weighted temperature in this region). With the assumption that the gas on large scales is in hydrostatic equilibrium with the gravitating dark matter, the gas and gravitating masses as a function of distance from the center of the cluster are shown in Figure 8.

We attempted to deproject the temperature and surface brightness profiles using the *project* model of XSPEC in order to determine the temperature and density as a function of distance from the nucleus. However, the statistical quality of these data was not sufficiently high to permit a detailed deprojection in this manner. We found that the deprojected temperature, density, and pressure profiles between $10''$ and $500''$ are statistically identical to the isothermal ($k_B T=3.4$ keV, $Z=0.5$) β -model profile. For simplicity, we will use the isothermal β -model profile parameters for energy and pressure comparisons with the radio lobes. The central hydrogen density, n_0 , of the isothermal β -model profile is 8.3×10^{-2} cm $^{-3}$. The gas pressure as a function of distance from the nucleus is shown in Figure 9.

We also made surface brightness profiles in four wedges, along the two jet axes (45° opening angle) and the two orthogonal axes (90° opening angle), to search for a surface brightness discontinuity that would indicate a detached shock. Such discontinuities have been observed in *Chandra* observations of the gaseous coronae of several radio galaxies including Hydra A (Nulsen *et al.* 2005), M87 (Forman *et al.* 2005), and MS 0735.6 + 7421 (McNamara *et al.* 2005). We find no statistically significant discontinuities in the surface brightness distribution along any of the axes.

3.3. Compact Components

A point source with an unusually soft spectrum is coincident with the active nucleus. We fit a power law model with Galactic absorption in the 0.5-2.0 keV band to the events within $2''$ of the nucleus (there are few source counts above 2 keV or below 0.5 keV). The

best-fit photon index is 2.9 ± 0.6 (90% confidence). Background was estimated in two ways: from a distant region and in an annulus around the nucleus. The results are insensitive to the choice of background. The unabsorbed luminosity is 2.7×10^{42} ergs s^{-1} in the 0.1-10.0 keV band. The X-ray to radio flux ratio lies along the correlation found for samples of radio galaxy cores (Canosa *et al.* 1999; Evans 2005). We also fit an APEC model with Galactic absorption to investigate whether the emission peak at the nucleus could be cold gas from the galaxy with high elemental abundance. Both the temperature and elemental abundance were free parameters in this fit. The thermal model was rejected at $>99\%$ confidence.

No X-ray emission is detected from the jet or the compact hotspot of the western lobe. The 3σ upper limit to the flux density of the western hotspot is 5.5×10^{-16} ergs $cm^{-2} s^{-1} keV^{-1}$ (0.23 nJy) at 1 keV, assuming a power-law spectrum with photon index 2.0. The lower limit to the radio-to-X-ray flux density spectral index is $\alpha_{rx} > 1.06$ based on an extrapolation from the 8.4 GHz flux density to the X-ray upper limit. The upper limit to the X-ray flux is two orders of magnitude above the expected value for inverse Compton scattering of CMB photons or from the SSC process assuming equipartition (Hardcastle, Birkinshaw & Worrall 1998). The limit on the X-ray to radio flux ratio of the hotspot is a factor of ten below that measured for the detected 3C 403 E hotspot (Hardcastle, Harris, Worrall, & Birkinshaw 2004; Kraft *et al.* 2005). There is thus not an unusually large population of ultra-relativistic, X-ray synchrotron emitting particles generated in this hotspot, which is consistent with what has been observed in the majority of FR II hotspots.

3.4. Sub-cluster merger

An X-ray enhancement $5'$ (~ 500 kpc) East of the cluster center may be a subcluster that is either falling toward 3C 388 or has already passed through the cluster core. Unfortunately the ACIS-I chip gaps lie directly across the bridge between the primary cluster and the sub-cluster, complicating an assessment of their relationship. An adaptively smoothed, background subtracted, exposure corrected image of this subcluster in the 0.5-2.0 keV band is shown in Figure 10. The morphology of this region is roughly triangular with diffuse peaks of X-ray emission at each vertex. One vertex is pointed away from the cluster center. The only known galaxy within $1'$ of this subcluster is 2MASX J18442603+4532219, which lies at the western boundary of the X-ray enhancement as shown in Figure 10, and is not associated with any of the X-ray peaks. There is no redshift reported in the literature for this object, although it appears to be two merging galaxies in the 2MASS images. This pair is approximately 2 magnitudes fainter than the host galaxy of 3C 388 in the K band. The temperature of the gas in the subcluster is $1.9_{-0.7}^{+2.1}$ keV assuming $Z=0.5Z_{\odot}$, and the

X-ray luminosity is 1.7×10^{42} ergs s^{-1} (within a $50''$ radius circle) in the 0.1-10.0 keV band assuming that it lies at the distance of the 3C 388 cluster. The quality of the data is not sufficient to conclusively determine whether this subcluster is falling toward 3C 388, is an unrelated foreground or background object, or has already passed through the cluster core. If the latter hypothesis is correct, the subcluster passed through the core ~ 500 Myrs ago (assuming a velocity of 1000 km s^{-1}), roughly an order of magnitude larger than the age of the radio source (see below). In this case, the merger will have deposited considerable energy in the core.

4. Interpretation

Our measurements of the thermodynamic parameters of the ICM permit us to make quantitative statements about the dynamics and energetics of the lobe inflation. Based on considerations of the jet/counterjet brightness, Leahy & Gizani (2001) estimate the jet makes an angle of $\sim 50^\circ$ with respect to the line of sight. This conclusion is supported by several lines of evidence including the axial ratio of the lobes and approximate equality of the Faraday depths of the lobes. For consistency, we use this estimate here. Our results below are not strongly dependent to this choice.

4.1. Hydrodynamics of buoyant hot bubbles

The surface brightness decrements and X-shaped morphology of the X-ray emission around the radio lobes indicate that the lobes have evacuated cavities in the gas. It is believed that the lobes of all radio galaxies are greatly overpressurized relative to the ambient medium early in their life (Reynolds, Heinz, & Begelman 2001). However, as discussed above, there is no evidence for sharp surface brightness discontinuities or large changes in gas temperature that would indicate strong shocks. If thermal conduction in the ICM is efficient (i.e. at or near the Spitzer value), shocks may be nearly isothermal and difficult to detect (Fabian *et al.* 2005a,b). However, *Chandra* observations the contact discontinuity in cluster ‘cold-fronts’ (Vikhlinin, Markevitch, & Murray 2001) and the high Mach number shock around the SW radio lobe of Centaurus A (Kraft *et al.* 2003, 2005b) suggest that the thermal conduction (and viscosity) of the ICM is orders of magnitude below the Spitzer value. Therefore, we conclude that the lobes are inflating transonically or subsonically (i.e. $M \leq 1$). This also suggests that the lobe are at most only moderately overpressurized relative to the ambient medium (factor of 2 at most (Landau & Lifshitz 1989)). Once the lobes reach pressure equilibrium with the ICM, their motion will be driven by buoyancy (Chura-

zov *et al.* 2002). We note that if the lobes are expanding supersonically, our conclusions regarding the energetics and dynamics of the lobes would be strengthened as we will have underestimated the energy of the outburst and overestimated the age of the lobes.

We assume that the lobes are in the buoyant stage to estimate their velocity of expansion and the age of the source. The expansion of the lobes was faster in the past, so our estimate of the age of the source will be an upper limit. We approximate the age of the bubble as the radius of the bubble divided by the buoyant velocity. The velocity of a buoyant bubble can be estimated by equating the buoyancy force with the drag (ram pressure). In this case, the velocity of the bubble is given by

$$v = \sqrt{g \frac{V}{S} \frac{2}{C}}, \quad (1)$$

where g is the acceleration of gravity, V and S are the volume and cross-section of the bubble, respectively, and C is the drag coefficient. The drag coefficient is a function of both the geometry and the Reynolds number, R , and is of order unity for R in the range of 10^3 to 10^5 . We assume that there is a large difference between the mass density of the lobe, ρ_{lobe} , and the ambient medium, ρ_{ICM} (i.e. $\rho_{lobe}/\rho_{ICM} \ll 1$).

Churazov *et al.* (2002) and Brüggén *et al.* (2002) estimate the drag coefficient for the buoyant radio bubbles in M87 using hydrodynamical arguments and numerical simulations. They conclude that $C \sim 0.7$ and $v \sim 0.6 \times c_s$. A similar calculation using the parameters of 3C 388 shows that $v \sim 0.9 \times c_s$. This is probably an overestimate for three reasons. First, the drag coefficient increases considerably for flows near Mach 1 (e.g. at $M=1$, C is roughly 4 times larger than for $M \ll 1$) due to the dissipative effect of weak shocks. Second, if the viscosity of the ISM is the Spitzer value (Spitzer 1962), the Reynolds number of the flow in 3C 388 is ~ 70 , considerably lower than the flows considered by Churazov *et al.* (2002) and Brüggén *et al.* (2002). The drag coefficient increases as R decreases for $R < 10^3$ (Figure 34 of Landau & Lifshitz (1989)). For a solid sphere rising buoyantly in a fluid with $R=70$, the drag coefficient, C , is 1.2. Third, the simple model of balancing the buoyant force and the drag is probably not a good approximation. The radius of the lobes is of the order of the distance of the lobes from the nucleus, and the effect of the compressibility of the lobes and the ambient gas, must be considered. The drag would be larger than estimated above in a detailed model that included a more complex geometry and compressibility of the gas. We therefore conservatively estimate $v \sim 0.5 c_s$, with an uncertainty of perhaps a factor of two, and thus estimate the age of the lobes as ≤ 65 Myrs.

We model each lobe as a cylinder with the axis parallel to and perpendicular to the jet axis for the East and West lobes, respectively, to estimate the volume of the lobes. Assuming the same geometry as above (i.e. the lobes lie at an angle of 50° with respect to the line of sight) and the best-fit β -model distribution for the gas, we estimate the ‘bubble’ enthalpy

(that is, the work done on the gas by the inflation of the lobe plus the internal energy of the lobe, $4pV$ for $\gamma=4/3$) to be 5.2 and 6.9×10^{59} ergs for the E and W lobes, respectively. The total mechanical energy of the AGN outburst therefore is 1.2×10^{60} ergs, of which 3.0×10^{59} ergs has already gone into work done on the cluster gas.

The inflation of the lobes has already added a significant amount of energy to the cluster core. The total thermal energy of the gas within the radius of the radio lobes is 1.8×10^{60} ergs. The work done on this gas by the lobes is 3.0×10^{59} ergs, or ~ 0.8 keV per particle. This estimate probably overestimates the heating per particle because the heat input has already spread beyond the region occupied by the lobes. If the lobes are currently evolving buoyantly, and hence subsonically, as we have argued above, the effect of the input heat will have propagated into the ambient ISM at the sound speed of the gas, or roughly twice the inflation velocity of the lobe. The energy has been input to a much larger volume of gas. Assuming the input energy has been added uniformly to the gas within twice the radius of the lobes, $2 \times R_{lobe}$, the amount of energy added is only 0.3 keV per particle.

It is likely that we are witnessing the ongoing quenching of a cluster cooling flow by a nuclear outburst. The temperature of the gas in the cluster core must have been ~ 0.3 keV cooler before the outburst than at present (assuming the heat has been uniformly distributed). For the current 3.5 keV gas temperature at the cluster center, the gas cooling time, $\tau_c \sim E_t/\epsilon$, where E_t is the thermal energy density of the gas and ϵ is the emissivity, is ~ 1 Gyr. If the gas in the cluster core were cooler, and therefore presumably denser, before the radio outburst, its radiative cooling time would have been considerably shorter, and it is likely that there was a significant accumulation of cooler gas. It is also probable that the cluster core is still reacting to the energy deposited by the inflation of the lobes. The gas in the cluster core is probably not in hydrostatic equilibrium in the gravitational potential. Depending on where the energy from the inflation of the lobes is ultimately deposited (i.e. in the cooling core or farther out in the halo), a temperature inversion may be created (i.e. the core may become hotter than the halo) in which case the gas would become convectively unstable.

The fossil group ESO 3060170 may be an example of a much later stage of a similar evolutionary process (Sun *et al.* 2004). *Chandra* and XMM-Newton observations demonstrated that there is no group scale cooling core in this group, although the radiative cooling time of the gas was much less than the Hubble time. It was suggested that a powerful radio outburst with total energy of a few $\times 10^{59}$ ergs (i.e. roughly comparable to what we have observed in 3C 388) may have reheated the cooling gas and quenched the cooling flow. There is no evidence for cavities in the gas in ESO 3060170, so any bubbles have presumably risen buoyantly into the halo and dispersed.

The amount of heating in the cluster could ultimately be significantly larger than ~ 0.3 keV per particle for three reasons. First, the initial stage of the bubble inflation was probably supersonic (Reynolds, Heinz, & Begelman 2001). A considerable amount of energy above the bubble enthalpy could have been added to the gas during this stage. Second, the bubble enthalpy will eventually be converted to thermal energy of the gas as the bubble rises in the atmosphere (Churazov *et al.* 2002). The enthalpy of the bubble is converted to kinetic energy of the gas as it falls in behind the rising bubble, then ultimately thermalizes into internal energy of the gas. The scale height to which the bubble will rise and within which the energy deposition takes place is uncertain and depends on several factors including how much ambient gas is entrained in the buoyantly rising bubble and whether or not the bubble remains adiabatic. In the case of Hydra A and Perseus A, the bubbles are likely to deposit at least half of their enthalpy into thermal energy of the gas within the cooling radius (Nulsen *et al.* 2002; Bîrzan *et al.* 2004). Finally, the jets and lobes are currently still powered by the active nucleus. Depending on how much longer the outburst lasts, the energy deposited in the gas could be a factor of a few larger than the current bubble enthalpy.

The rate at which the mechanical power is deposited into the gas is the pV work divided by the inflation time of the lobe or $\sim 4 \times 10^{44}$ ergs s^{-1} . This is two orders of magnitude greater than the current radiative power output of the active nucleus, and is not atypical compared to other radio galaxies/cluster cavities that have been studied in detail. A sample of 18 X-ray cavities in clusters, groups, and galaxies has been studied from data in the *Chandra* archive (Bîrzan *et al.* 2004) where it was found that the ratio between the mechanical power of the outburst and the radiative power of the AGN or the radio luminosity of the lobes varied between factors of ten to several hundred. The large difference between the mechanical power and the radio power of radio galaxies was predicted on theoretical grounds (De Young 1993; Bicknell, Dopita, & O’Dea 1997). As discussed by Owen *et al.* (2000) and Bîrzan *et al.* (2004), the radio power of a radio galaxy is not a good indicator of the mechanical power of the outburst.

The energy input by the inflation of the lobes is more than sufficient to balance radiative losses in the core. We define the cooling radius, r_{rad} as the distance from the nucleus where the cooling time is 5 Gyrs (33.4 kpc for 3C 388). This is roughly the distance at which radiative losses must be balanced by another source of energy. The cooling time of 5 Gyrs roughly corresponds to the time between major merger events. Within this radius, the X-ray luminosity is 2.2×10^{43} ergs s^{-1} (unabsorbed) in the 0.1-10.0 keV band. This is roughly a factor of 20 less than the lower limit to the rate of mechanical energy deposition of the current outburst. If the duty cycle of outbursts of the observed magnitude is only 5%, the accumulation of cooling gas at the cluster center will be quenched. Our results are consistent with hydrodynamic simulations of cyclical nuclear outbursts in galaxy clusters. Dalla Vecchia

et al. (2004) demonstrate that repetitive outbursts with mechanical power similar to 3C 388 with a duty cycle of 5-10% can suppress the formation of cooling gas.

If the interpretation of Roettiger *et al.* (1994) for 3C 388 is correct and the differences in radio spectral index of the radio lobes indicates multiple outbursts, the picture is somewhat more complicated. Assuming that 3C 388 is not an X-shaped radio galaxy seen in projection (Leahy & Williams 1984; Kraft *et al.* 2005), the more recent radio outburst has ‘caught-up’ with the older outburst and implies near transonic velocities. The older outburst must be evolving buoyantly, and if the more recent outburst has displaced the older bubble, then the lobes are inflating transonically and perhaps supersonically. This would have several important implications. First, our estimate of the evolutionary timescale of the bubble would be reduced by a factor of four or more, with a consequent increase in the rate of mechanical energy deposition by the same factor. The discrepancy between the current luminosity of the AGN and the time averaged rate of mechanical work to inflate the lobe becomes even larger. Second, we will have considerably underestimated the total energy deposited into the cooling flow. The older outburst must also have deposited a similar amount of energy into the ICM (assuming a similar volume). In addition, transonic or supersonic inflation velocities imply that the hot ISM has been shock heated.

4.2. Internal pressure of radio lobe

The equipartition pressure of the diffuse regions of the radio lobes is $\sim 4 \times 10^{-12}$ dyn cm^{-2} based on GHz frequency radio measurements. Using the best-fit models of the β profile, and assuming that the jet/counterjet makes an angle of $\sim 50^\circ$ with respect to the line of sight, we estimate the thermal gas pressure at the approximate position of the lobes to be $\sim 7.0 \times 10^{-11}$ dyn cm^{-2} , more than an order of magnitude larger than the minimum pressure of the lobes. We conclusively confirm the results of Hardcastle & Worrall (2000) and Leahy & Gizani (2001) (based on ROSAT HRI observations) that the radio lobes are greatly underpressurized relative to the ambient medium. It is not feasible that the lobes are so underpressurized relative to the gas as they would be crushed in a sound crossing time if this were the case. Either the equipartition assumption is incorrect, or something else dominates the pressure of the lobes.

A significant difference between the equipartition pressure of lobes and jets in FR I radio galaxies and the pressure of the ambient medium has now been observed in a large number of sources and appears to be a common phenomenon (e.g. Croston *et al.* (2003); Dunn & Fabian (2004)). However, X-ray observations of inverse-Compton scattering of CMB photon from relativistic electrons in the radio lobes of FR II radio galaxies in poorer environments

than 3C 388 have demonstrated that the relativistic electrons responsible for the GHz radio emission are not far out of equipartition with the magnetic field (Hardcastle *et al.* 2002; Croston *et al.* 2005). Based on morphology and radio power, 3C 388 is classified as an FR II, yet the large difference between the equipartition pressure and the ambient medium is typical of FR Is. If the lobes of 3C 388 are not in equipartition but the GHz emitting particles and lobe magnetic field are in pressure equilibrium with the gas, either there is an excess of particles, or the field is stronger than the equipartition value. If the lobe is particle dominated, the magnetic field must be approximately 10% of the equipartition value to maintain pressure balance with the gas, which is well outside the distribution inferred from lobe IC emission by Croston, Birkinshaw, Hardcastle, & Worrall (2004). On the other hand, it is possible the lobes are magnetically dominated, but this is typically difficult to arrange.

There are several possible sources for this ‘missing’ pressure including lower energy relativistic electrons ($\gamma \sim 10$, which would radiate at kHz frequencies and be unobservable) or protons, partial filling factor of the relativistic gas, and entrained thermal protons. Each of these hypotheses has significant problems, however. If a population of lower energy relativistic electrons dominates the pressure, the magnetic field should come into equipartition with this. The fact that the field is close to equipartition with GHz-emitting charged particle population means that additional energetically dominant particle distributions are unlikely (Croston *et al.* 2005). The latter two possibilities are more difficult to rule out observationally. It is possible that the radio emitting plasma is clumpy, but as Leahy & Gizani (2001) point out, the filling factor would have to be extremely low ($\sim 1\text{-}2\%$) to retain equipartition. It is also possible that thermal gas has been entrained into the lobe via Kelvin-Helmholtz instabilities. The visibility of the X-ray cavity suggests that such plasma, if present, must be considerably hotter and less dense than the ambient ICM. The entrained gas could then be heated via thermal conduction by the relativistic plasma in the lobe. No such hot gas has been detected in any radio lobe, and the temperature of this gas would have to be high (>15 keV) for it not to be visible in nearby radio galaxies with *Chandra* (Nulsen *et al.* 2002; Schmidt, Fabian, & Sanders 2002). Mazotta *et al.* (2002) discovered a hot ($T \sim 7.5$ keV) bubble of gas in the cluster MKW 3s that appears as a surface brightness deficit in the *Chandra* image. There is no radio emission associated with this X-ray bubble, and whether it is the result of the entrainment and heating of the ICM gas during the inflation of a radio lobe is unknown.

5. Conclusions

We detect cavities in the X-ray emission from the cluster gas coincident with the radio lobes of 3C 388. There is no evidence for temperature or surface brightness discontinuities suggestive of strong shocks in the gas. Thus the lobes must be evolving transonically or subsonically. The work done by the inflation of the lobes on the gas is at least 0.3 keV per particle out to twice the radius of the lobe. The bubble enthalpy, when ultimately converted to thermal energy of the gas, will increase this by a factor of a few. The rate of mechanical energy deposition by the inflation of the lobes is at least twenty times greater than the radiative power of the ICM within the cooling radius. Thus, repeated outbursts of similar power with a duty cycle of only a few percent are more than capable of suppressing the accumulation of cool gas at the core of this cluster of galaxies. Because of the large difference between the mechanical power input into the gas by the inflation of the lobes and the radiative losses, this is one of the best examples of the quenching of cooling gas by a nuclear outburst.

The equipartition pressure of the lobes is more than an order of magnitude less than the pressure of the ambient medium. The pressure of the lobes must therefore be dominated by something other than the relativistic particles emitting at GHz radio frequencies. In this regard, the lobes of 3C 388 are more similar to the plumes and lobes of FR I radio galaxies than to the lobes of FR II sources (at least those in poor environments).

This work was supported by NASA contracts NAS8-38248, NAS8-39073, the Royal Society, the Chandra X-ray Center, and the Smithsonian Institution. We thank the anonymous referee for comments that improved this paper.

REFERENCES

- Anders E. & Grevasse N. 1989, *Geochimica et Cosmochimica Acta*, **53**, 197.
- Basson, J. F., & Alexander, P. 2003, *MNRAS*, **339**, 353.
- Bicknell, G. V., Dopita, M. A., & O’Dea, C. P. 1997, *ApJ*, **485**, 112.
- Birzan, L., Rafferty, D. A., McNamara, B. R., Wise, M., W., & Nulsen, P. E. J. 2004, *ApJ*, **607**, 800.
- Böhringer, H., & Morfill, G. E. 1988, *ApJ*, **330**, 609.
- Brüggen, M., Kaiser, C. R., Churazov, E., & Enßlin, T. A. 2002, *MNRAS*, **331**, 545.
- Canosa, C. M., Worrall, D. M., Hardcastle, M. J., Birkinshaw, M. 1999, *MNRAS*, **310**, 30.
- Churazov, E., Sunyaev, R., Forman, W., & Böhringer, H. 2002, *MNRAS*, **332**, 729.
- Croston, J. H., Hardcastle, M. J., Birkinshaw, M., Worrall, D. M. 2003, *MNRAS*, **346**, 1041.
- Croston, J. H., Birkinshaw, M., Hardcastle, M. J., & Worrall, D. M. 2004, *MNRAS*, **353**, 879.
- Croston, J. H., Hardcastle, M. J., Harris, D. E., Belsole, E., Birkinshaw, M., & Worrall, D. M. 2005, *ApJ*, **626**, 733.
- Dalla Vecchia, Claudio, Bower, Richard G., Theuns, Tom, Balogh, Michael L., Mazzotta, Pasquale, & Frenk, Carlos S. 2004, *MNRAS*, bf 355, 995.
- De Young, D. S. 1993, *ApJ*, **405**, L13.
- Dickey, J. M., & Lockman, F. J. 1990, *ARA&A*, **28**, 215.
- Dolag, K., Jubelgas, M., Springel, V., Borgani, S., & Rasia, E. 2004, *ApJ*, **606**, L97.
- Dunn, R. J. H., & Fabian, A., C. 2004, *MNRAS*, **355**, 862.
- Evans, D. 2005, Ph.D. dissertation, University of Bristol.
- Evrard, A. E., Metzler, C. A., & Navarro, J. F. 1996, *ApJ*, **469**, 494.
- Fabian, A. C., Reynolds, C. S., Taylor, G. B., & Dunn, R. J. H. 2005, *MNRAS*, **363**, 891.
- Fabian, A. C., Sanders, J. S., Taylor, G. B., Allen, S. W., Crawford, C. S., Johnstone, R. M., & Iwasawa, K. 2005, *astro-ph/0510476*.

- Fanaroff, B. L., & Riley, J. M. 1974, MNRAS, **167**, 31p.
- Feigelson, E. D. & Berg, C. J. 1983, ApJ, **269**, 400.
- Finoguenov, A. & Jones, C. 2001, ApJ, **547**, L107.
- Forman, W. R. *et al.* 2005, ApJ, in press.
- Hardcastle, M. J., Birkinshaw, M., & Worrall, D. M. 1998, MNRAS, **294**, 615
- Hardcastle, M. J. & Worrall, D. M. 1999, MNRAS, **309**, 969.
- Hardcastle, M. J. & Worrall, D. M. 2000, MNRAS, **319**, 562.
- Hardcastle, M. J., Birkinshaw, M., Cameron, R. A., Harris, D. E., Looney, L. W., & Worrall, D. M. 2002, ApJ, **581**, 948.
- Hardcastle, M. J., Harris, D. E., Worrall, D. M., and Birkinshaw, M. 2004, ApJ, **612**, 729.
- Jackson, N., & Rawlings, S. 1997, MNRAS, **286**, 241.
- Jones, C. *et al.* 2002, ApJ, **567**, L115.
- Kaastra, J. S., *et al.* 2004, A. & A., **413**, 415.
- Kraft, R. P., Vazquez, S. E., Forman, W. R., Jones, C., Murray, S. S., Hardcastle, M. J., Worrall, D. M., Churazov, E. 2003, ApJ, **592**, 129.
- Kraft, R. P., Hardcastle, M. J., Worrall, D. M., & Murray, S. S., ApJ, **622**, 149.
- Kraft, R. P., *et al.* 2005, in preparation.
- Landau, L. D., & Lifshitz, E. M. 1989, 'Fluid Mechanics', 2nd ed., Butterworth and Heinemann.
- Leahy, J. P., & Williams, A. G., MNRAS, **210**, 929.
- Leahy, J. P., & Gizani, N. A. B. 2001, ApJ, **555**, 709.
- Martel, A. R., *et al.* 1999, ApJS, **122**, 81.
- Mazzotta, P., Kaastra, J. S., Paerels, F. B., Ferrigno, C., Colafrancesco, S., Mewe, R., & Forman, W. R. 2002, ApJ, **567**, L37.
- McNamara, B. R., *et al.* 2000, ApJ, **534**, L135.

- McNamara, B. R., Wise, M. W., & Murray, S. S. 2004, *ApJ*, **601**, 173.
- McNamara, B. *et al.* 2005, *Nature*, **433**, 45.
- Nulsen, P. E. J., David, L. P., McNamara, B. R., Jones, C., Forman, W. R., & Wise, M. 2002, *ApJ*, **568**, 163.
- Nulsen, P. E. J., McNamara, B. R., Wise, M. W., & David, L. P. 2005, *ApJ*, **628**, 629.
- Owen, F. N. & Laing, R. A. 1989, *MNRAS*, **238**, 357.
- Owen, F. N., Eilek, Jean A., & Kassim, Namir E. 2000, *ApJ*, **543**, 611.
- Peterson, J. R., *et al.* 2001, *ApJ*, **590**, 207.
- Prestage, R. M., & Peacock, J. A. 1998, *MNRAS*, **230**, 131.
- Reynolds, C. S., Heinz, S., and Begelman, M. C. 2001, *ApJ*, **569**, L79.
- Reynolds, C. S., Heinz, S., and Begelman, M. C. 2002, *MNRAS*, **332**, 271.
- Roettiger, K., Burns, J. O., Clarke, D. A., & Christiansen, W. A. 1994, *ApJ*, **421**, L23.
- Schmidt, R. W., Fabian, A. C., & Sanders, J. S. 2002, *MNRAS*, **337**, 71.
- Spergel, D., *et al.* 2003, *ApJS*, **148**, 175.
- Spitzer, L. 1962, “Physics of Fully Ionized Gases”, John Wiley and Sons, New York.
- Sun, M., Forman, W., Vikhlinin, A., Hornstrup, A., Jones, C., and Murray, S. S. 2004, *ApJ*, **612**, 805.
- Tabor, G., & Binney, J. 1993, *MNRAS*, **263**, 323.
- Tucker, W. H., & Rosner, R. 1983, *ApJ*, **267**, 547.
- Vikhlinin, A., Markevitch, M., & Murray, S. S. 2001, *ApJ*, **549**, L47.

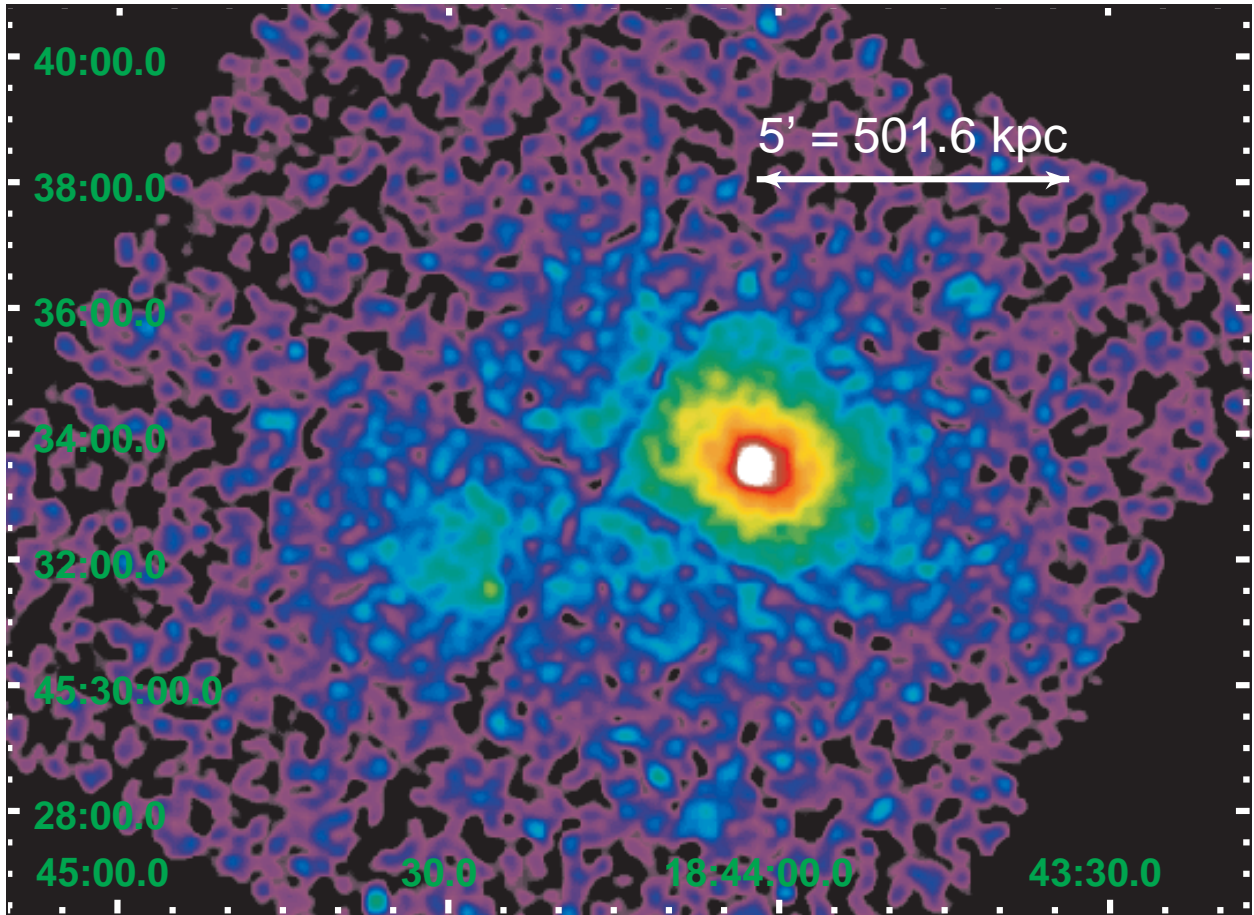


Fig. 1.— Gaussian smoothed ($6''$ r.m.s.) *Chandra*/ACIS-I image of 3C 388 in the 0.5-2.0 keV band with point sources removed.

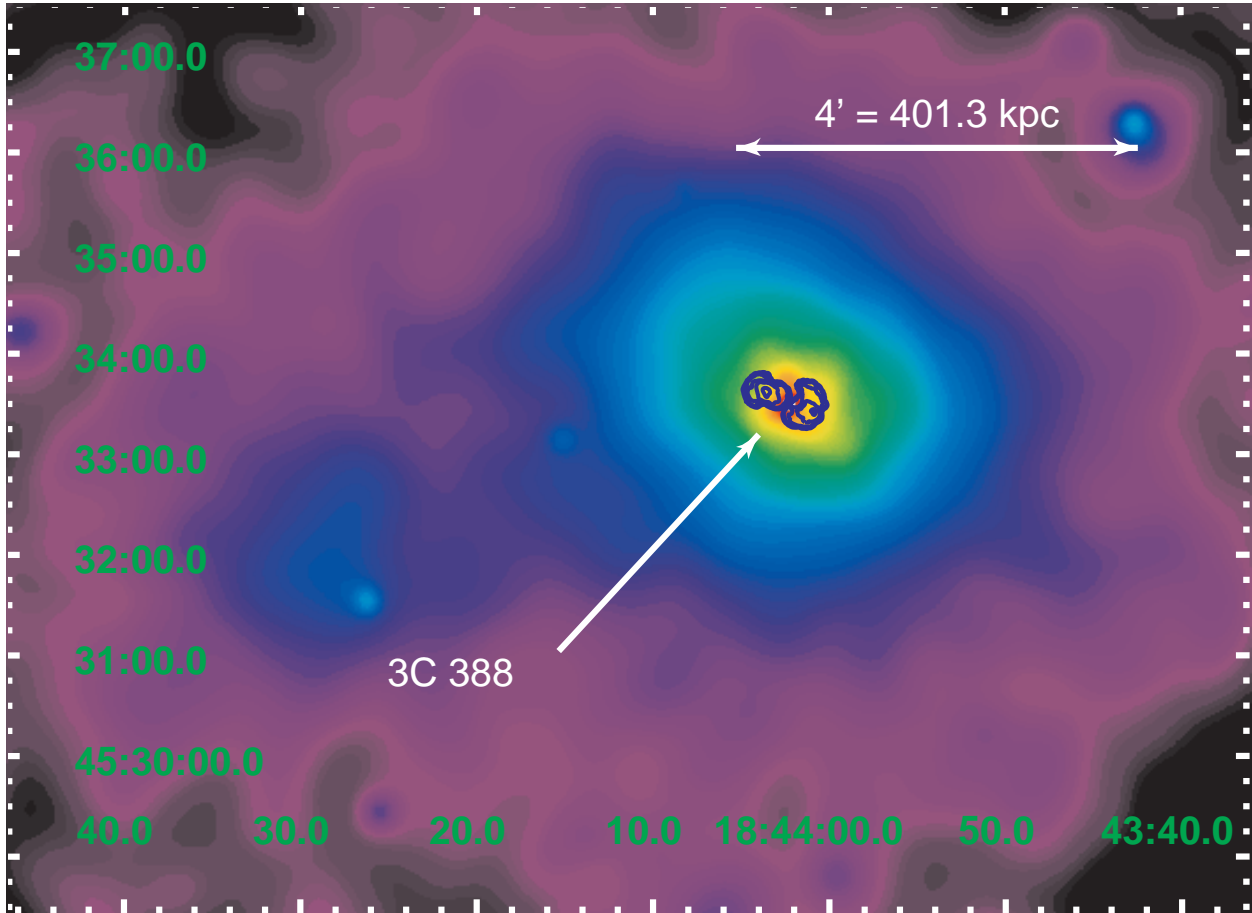


Fig. 2.— Adaptively smooth, background subtracted, exposure corrected *Chandra*/ACIS-I image of 3C 388 in the 0.5-2.0 keV band with 1.4 GHz radio contours overlaid (blue). The bright nucleus, ICM, and southeastern concentration are clearly visible.

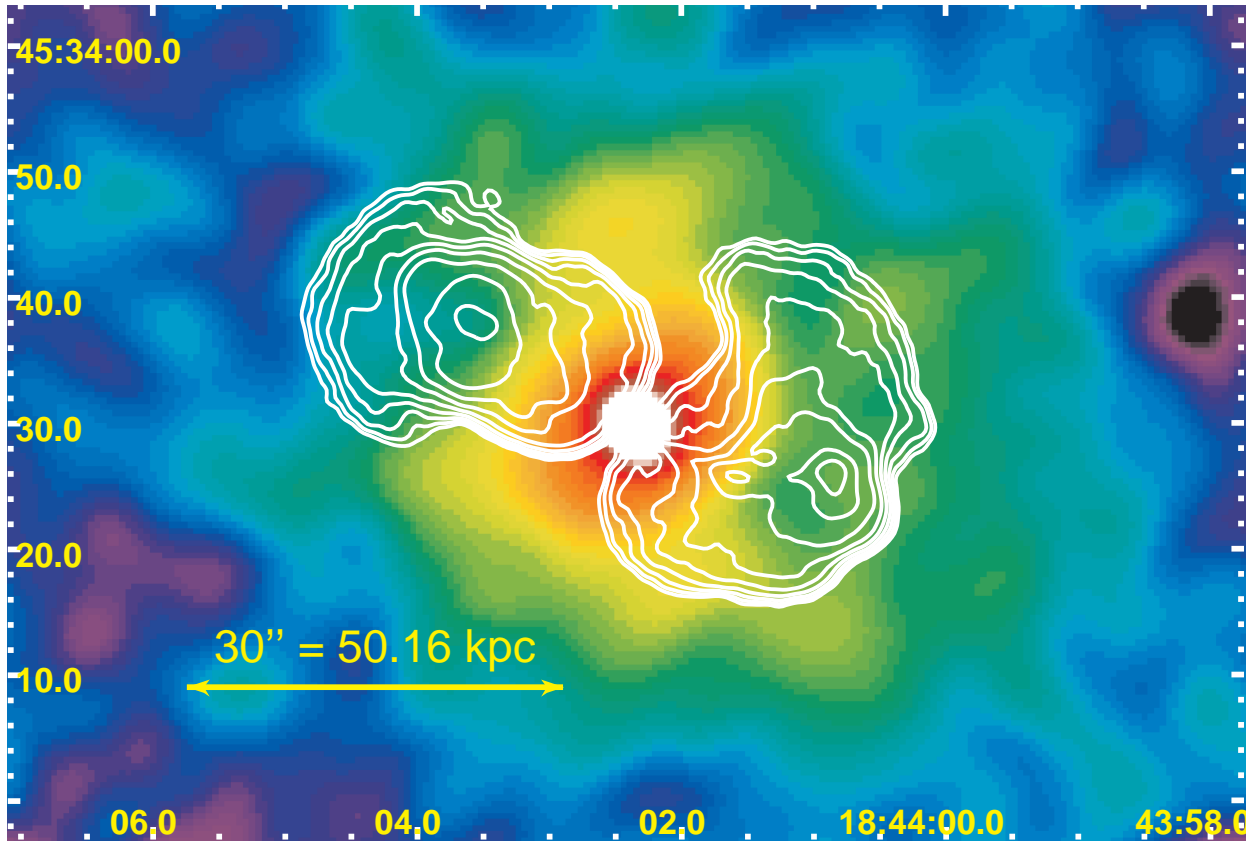


Fig. 3.— Adaptively smooth, background subtracted, exposure corrected *Chandra*/ACIS-I image of 3C 388 in the 0.5-2.0 keV band with 5 GHz radio contours overlaid.

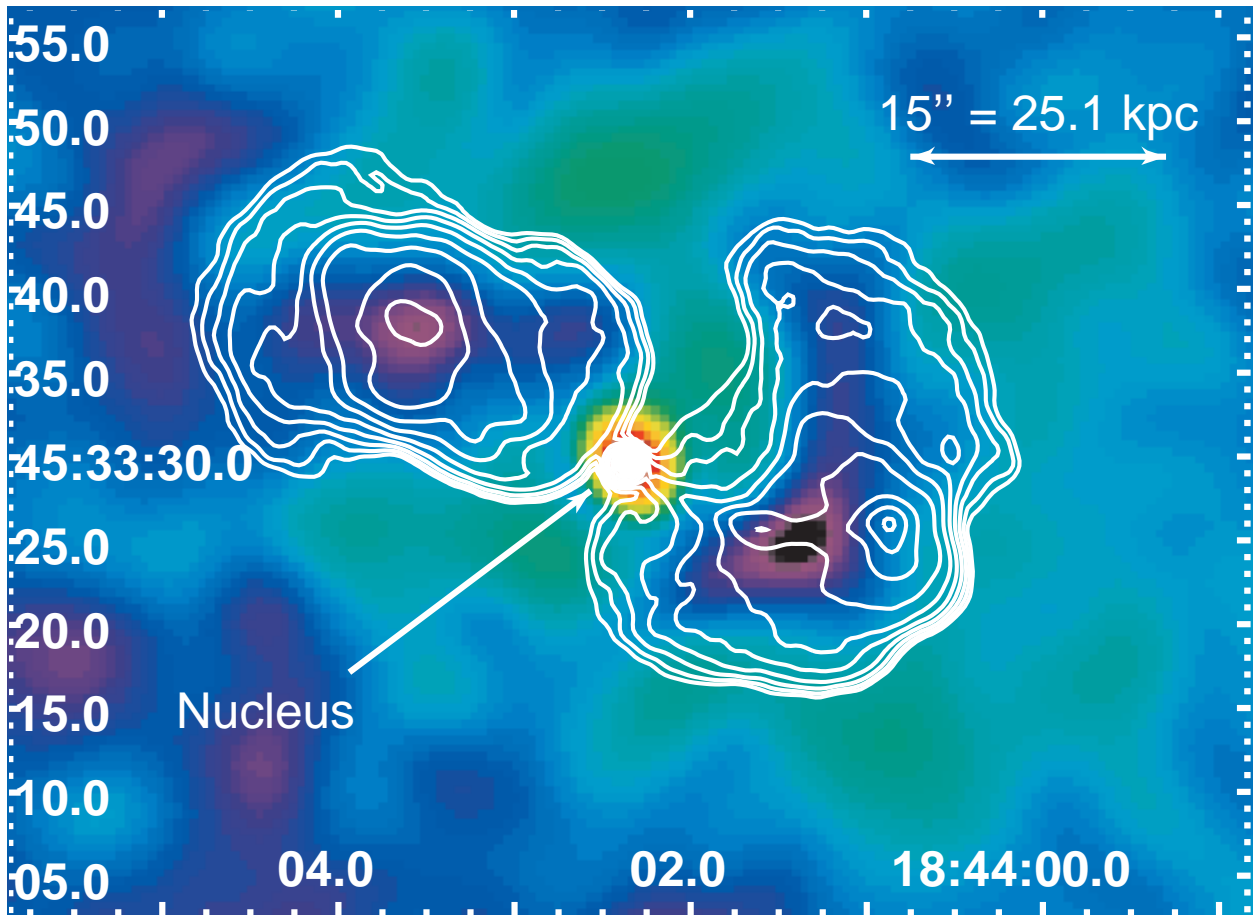


Fig. 4.— Smoothed ($2''$ Gaussian r.m.s.), background subtracted, exposure corrected *Chandra*/ACIS-I image of 3C 388 in the 0.5–2.0 keV band with azimuthal profile subtracted to enhance the appearance of the X-ray cavities associated with the radio lobes. Radio contours (1.4 GHz) are overlaid. The ‘peaks’ of the surface brightness decrements (shown as black at the center of the lobes) correspond to a $\sim 25\%$ decrease in the X-ray surface brightness relative to the azimuthal average.

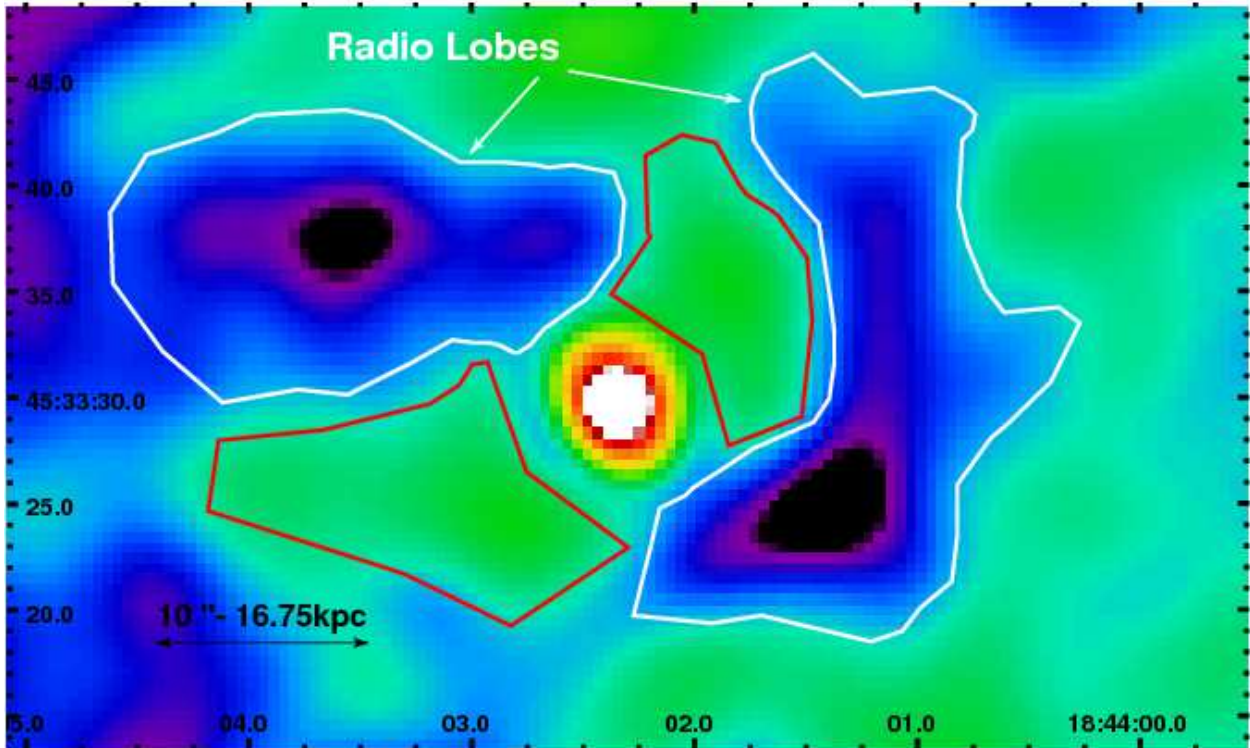


Fig. 5.— Regions extracted for spectral analysis. Region 1 is coincident with the radio lobes (white), region 2 is interior to the lobes (red), and region 3 is an elliptical annulus with inner and outer semi-major axes of $25''$ and $50''$, respectively. The best fit temperatures and abundances with 90% uncertainties are summarized in Table 1.

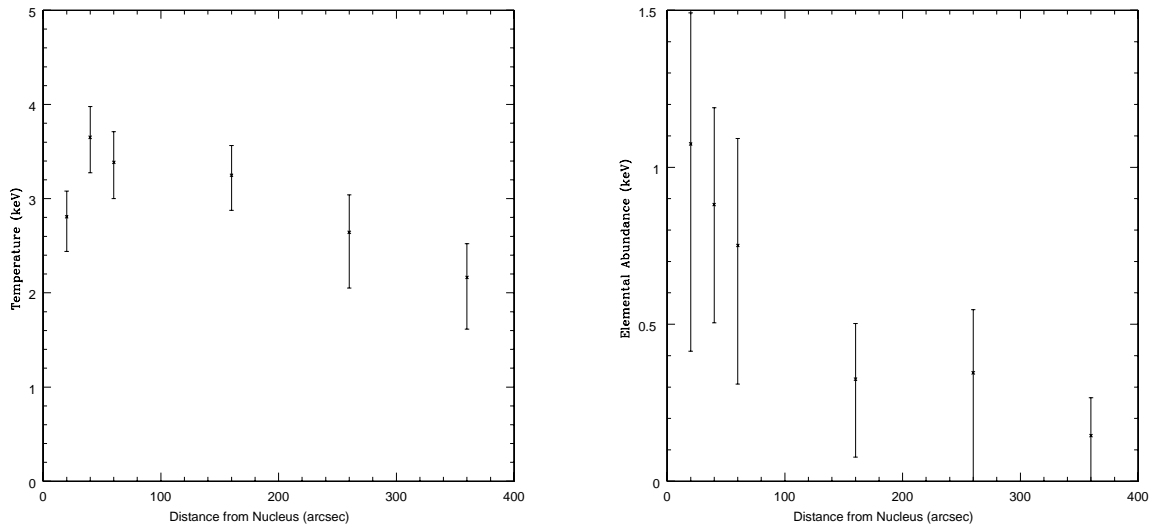


Fig. 6.— Radial temperature and elemental abundance profiles of the ICM around 3C 388 in azimuthal regions.

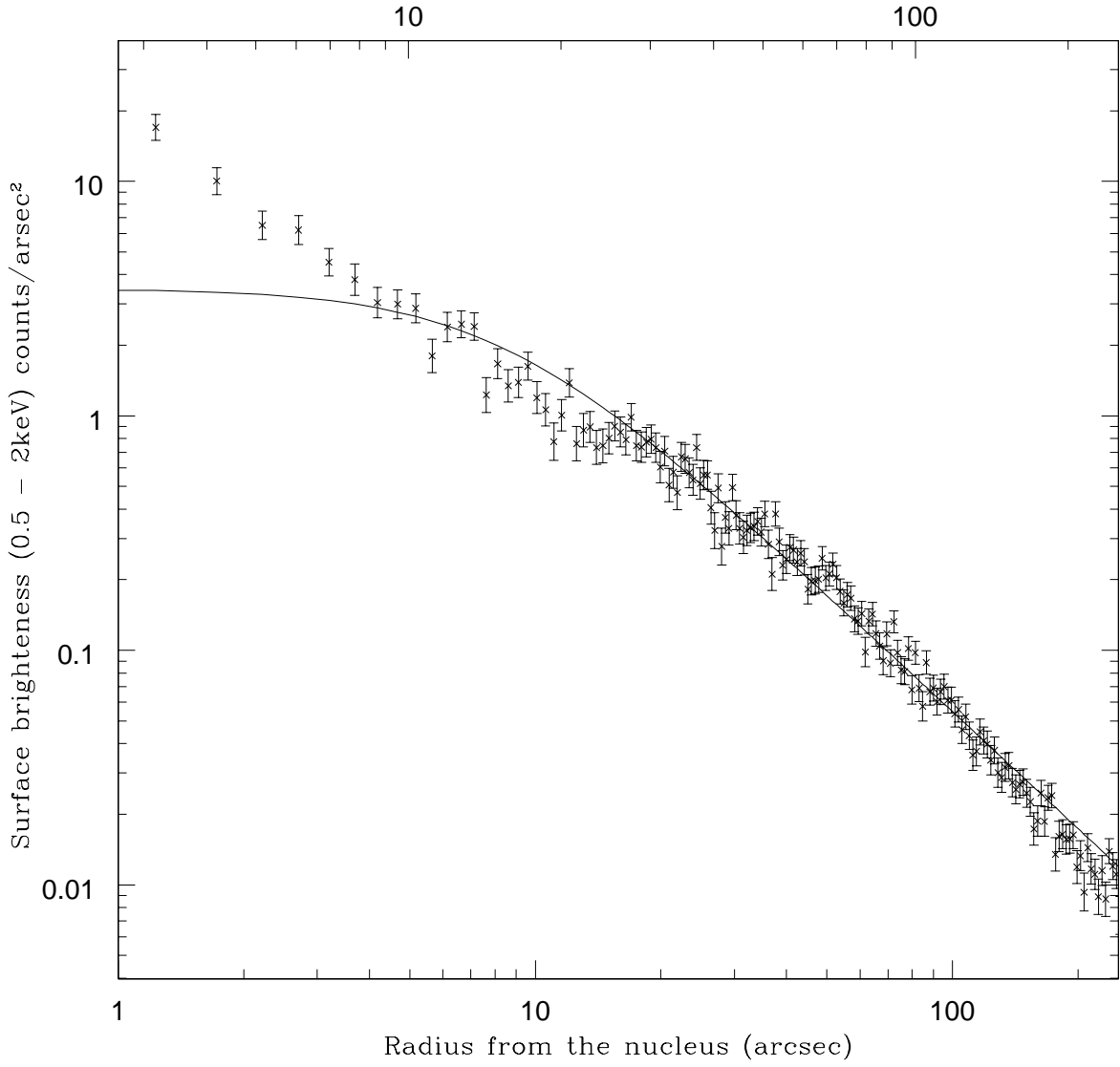


Fig. 7.— Radial surface brightness profile of ICM around 3C 388.

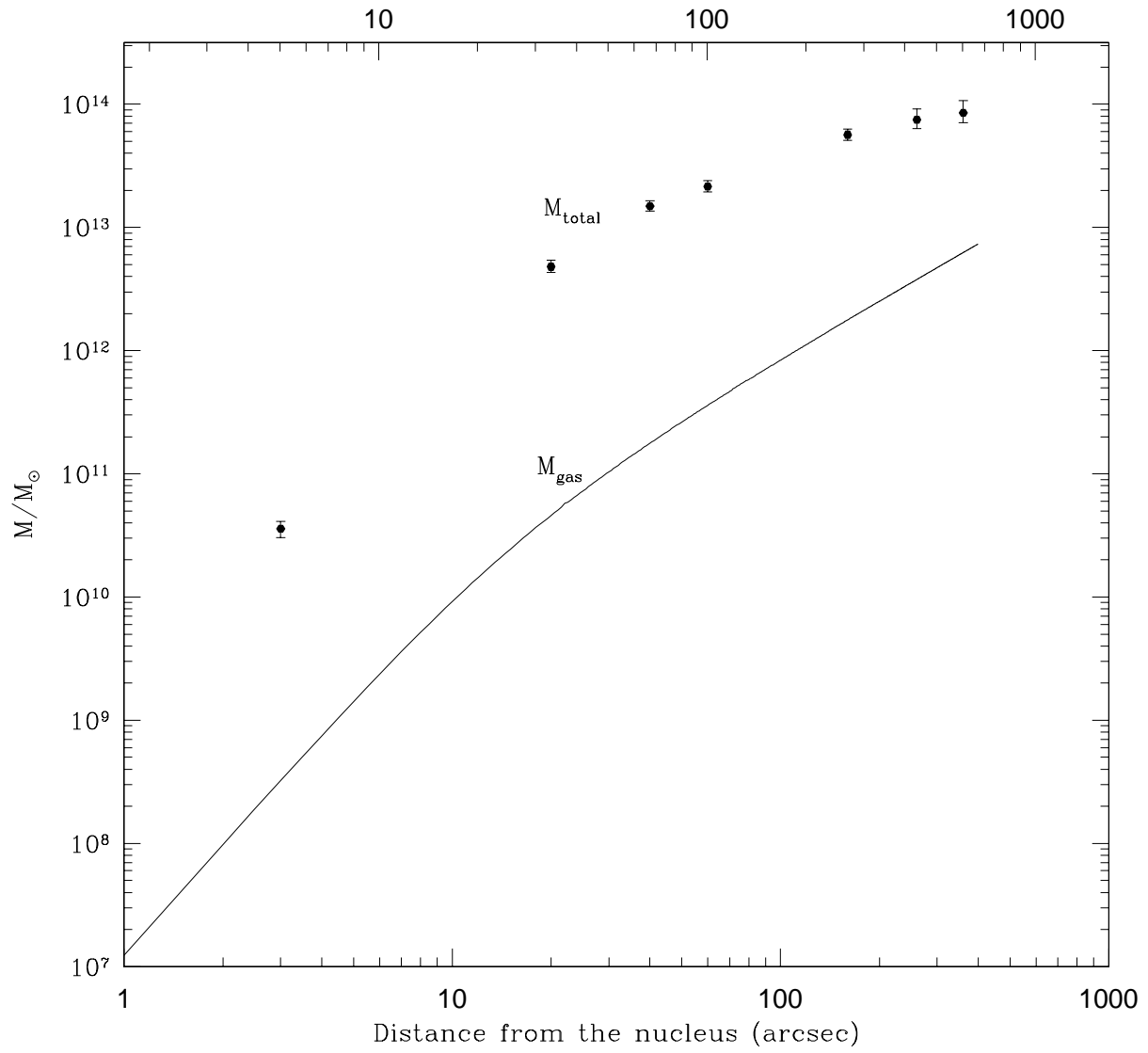


Fig. 8.— Gas mass and gravitating mass as a function of distance from the center of the cluster.

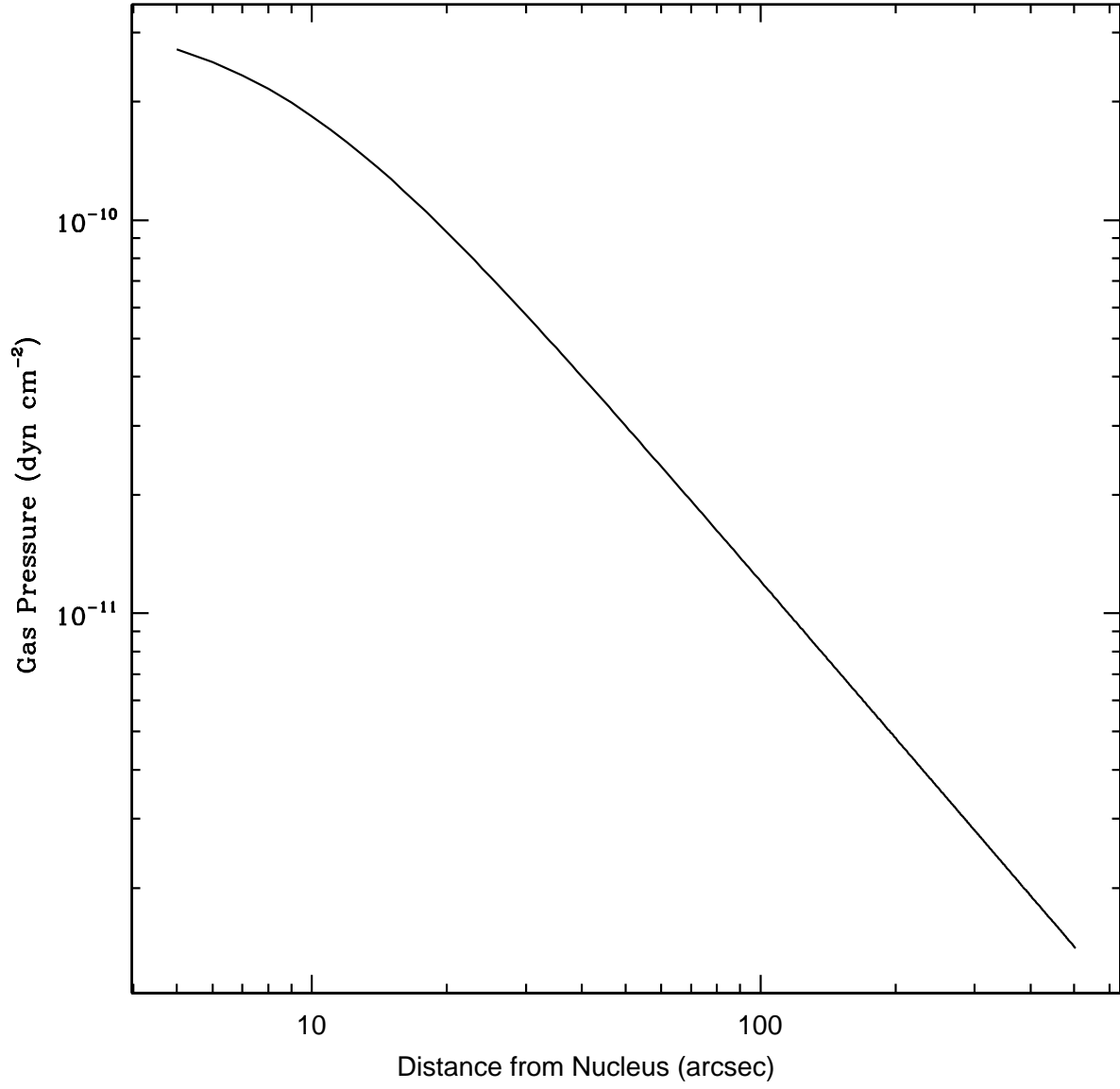


Fig. 9.— Gas pressure of the ICM as a function of distance from the nucleus for isothermal β -model profile.

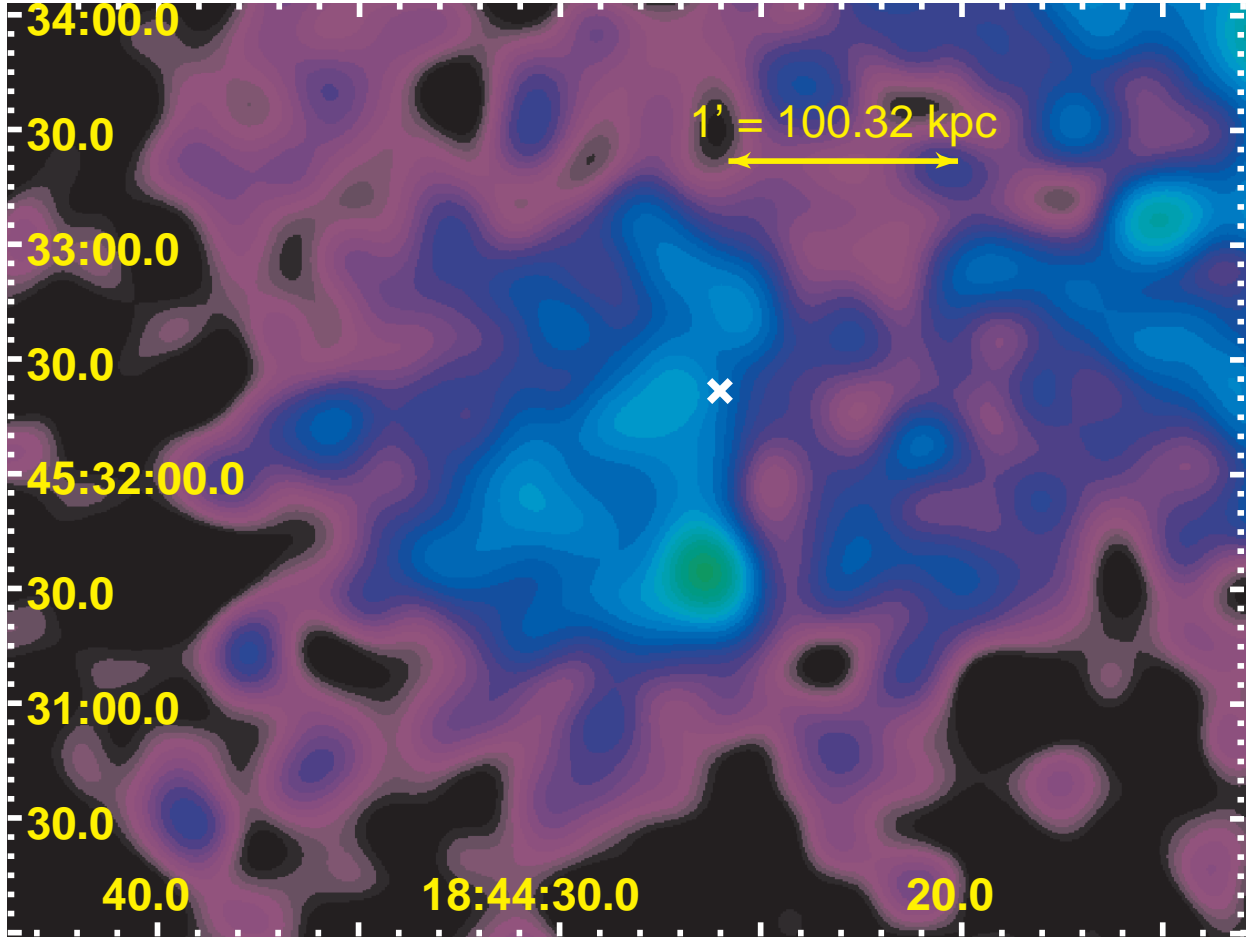


Fig. 10.— Adaptively smoothed, background subtracted, exposure corrected *Chandra*/ACIS-I image in the 0.5-2.0 keV band of the subcluster to the E of 3C 388. The white X corresponds to the position of the optical/IR galaxy 2MASX J18442603+4532219.

Region	Temperature (keV)	Abundance
1	$2.8^{+1.2}_{-0.7}$	$0.7^{+2.8}_{-0.6}$
2	$3.1^{+1.0}_{-0.8}$	$0.3^{+1.0}_{-0.3}$
3	$3.4^{+1.1}_{-0.7}$	$0.6^{+1.4}_{-0.4}$

Table 1: Summary of best fit temperatures and abundances (fraction of Z_{\odot}) in three regions around 3C 388. Uncertainties are at 90% confidence. See text (section 3.1) and Figure 5 for description of regions.